Interactions of localized wave structures and dynamics in the defocusing coupled nonlinear Schrödinger equations

Guoqiang Zhang,[1,2] Zhenya Yan,[1,2,*] Xiao-Yong Wen,[1,3] and Yong Chen[1,2]

[1]*Key Laboratory of Mathematics Mechanization, Institute of Systems Science, AMSS, Chinese Academy of Sciences, Beijing 100190, China*

[2]*School of Mathematical Sciences, University of Chinese Academy of Sciences, Beijing 100049, China*

[3]*Department of Mathematics, School of Applied Science, Beijing Information Science and Technology University, Beijing 100192, China*

(Received 25 November 2016; published 10 April 2017)

We investigate the defocusing coupled nonlinear Schrödinger equations from a 3×3 Lax pair. The Darboux transformations with the nonzero plane-wave solutions are presented to derive the newly localized wave solutions including dark-dark and bright-dark solitons, breather-breather solutions, and different types of new vector rogue wave solutions, as well as interactions between distinct types of localized wave solutions. Moreover, we analyze these solutions by means of parameters modulation. Finally, the perturbed wave propagations of some obtained solutions are explored by means of systematic simulations, which demonstrates that nearly stable and strongly unstable solutions. Our research results could constitute a significant contribution to explore the distinct nonlinear waves (e.g., dark solitons, breather solutions, and rogue wave solutions) dynamics of the coupled system in related fields such as nonlinear optics, plasma physics, oceanography, and Bose-Einstein condensates.

DOI: 10.1103/PhysRevE.95.042201

I. INTRODUCTION

The nonlinear Schrödinger (NLS) equation, as an important physical and completely integrable model, appears in many fields of science such as nonlinear optics [1–3], hydrodynamics [4], plasma physics [5], molecular biology [6], Bose-Einstein condensates [7], and even finance [8,9]. The focusing NLS equation has been shown to possess bright solitons with zero initial condition and breather solutions with plane-wave initial condition by using the inverse scattering method or Darboux transformation [10]. In particular, rogue wave (RW) solutions, as the parameter limits of breather solutions, of the focusing NLS equation had been presented in the rational form in 1983, which was also called the Peregrine soliton. Darboux transformation, originating from the work of Darboux in 1882 on the Sturm-Liouville equation, is a powerful method to derive some types of localized wave solutions of many nonlinear integrable systems [11]. More recently, higher-order RWs of the focusing NLS equation have been found by using the modified Darboux transformation [12,13]. Moreover, the nonautonomous rogue waves (rogons) were presented for the NLS equation and its extensions with varying coefficients [14]. After that, the generalized Darboux transformation [15] was used to investigate separable higher-order RW solutions of the focusing NLS equation and other nonlinear integrable equations [16]. Furthermore, another generalized perturbation Darboux transformation was also presented to find higher-order RW solutions of integrable nonlinear wave equations [17,18].

The regular rogue wave solutions of the defocusing NLS equation were not found yet since its rational solutions were shown to have the singular points up to now. The two-component NLS equations are of the more complicated structures than the scalar NLS equation since their Lax systems are distinct. The two-component focusing NLS equations have been shown to admit the vector RW solutions [9,19,20]. The two-component defocusing NLS equations have also been shown to admit the first-order vector RW solutions [21], which differ from the scalar defocusing NLS equation and may be due to the interactions of different components. Recently, the mixed two-component NLS equations have been shown to admit the RW solutions and dark-dark-rogue wave solutions by using the Darboux transformation [22].

In this paper, we consider the defocusing coupled nonlinear Schrödinger (dCNLS) equations in dimensionless form,

$$\begin{aligned} ip_t + p_{xx} - 2(|p|^2 + |q|^2)p = 0, \\ iq_t + q_{xx} - 2(|p|^2 + |q|^2)q = 0, \end{aligned} \tag{1}$$

where $p(x,t)$ and $q(x,t)$ denote the complex amplitudes of two wave packets and the subscripts stand for the partial derivative with respect to the variables. System (1) usually describes the pulse propagation in a long normally dispersive optical fiber with random birefringence [23,24]. System (1) can also modulate the interaction between waves of different frequencies and between orthogonally polarized components in nonlinear optical fibers [1,2,25]. System (1) was used to describe the electromagnetic wave propagation in isotropic and homogeneous nonlinear left-handed materials [26]. System (1) gave a suitable model for crossing sea waves within the hydrodynamics context [27]. Moreover, system (1) can also describe the evolution of a two-component Bose-Einstein condensate composed of different hyperfine states in the case of an elongated trap (the aspect ratio of the condensate is small enough and the densities of both components are low enough) [28,29].

System (1) should first be deduced by Benney and Newell [30] from two interacting nonlinear wave packets in a dispersive and conservative system. After that, Manakov [31] showed that system (1) was completely integrable. The dCNLS system has been shown to possess the fundamental exploration of complex coupled soliton dynamics (e.g., dark-dark and dark-bright soliton pairs) [32–38]. Recently, some first-order RWs of system (1) have been found using the Darboux-dressing construction [21,39]. However, it is still

*zyyan@mmrc.iss.ac.cn

an important subject to explore new wave structures (e.g., RWs and interactions of RWs and solitons) and to further study their dynamical behaviors. It is known that the Darboux transformation for the dCNLS equations is not positive or negative definite. In this work, we will extend the idea [22] to present a unified N-fold Darboux transformation such that generalized localized wave solutions and interactions between solitons, breather solutions, and RWs are found for the dCNLS equation (1).

This paper is organized as follows. In Sec. II, we present the N-fold Darboux transformation for the dCNLS equations. In Secs. III–V, we choose the plane-wave solutions as the seed solutions to find the new solutions of the dCNLS equations by means of the obtained N-fold Darboux transformation. These obtained solutions contain dark-dark and bright-dark solitons, breather-breather solutions, and different types of new vector rogue wave solutions, as well as interactions between distinct types of localized wave solutions. Moreover, we analyze these solutions by means of parameters modulation. In Sec. VI, we analyze some respective wave structures and their dynamical behaviors by means of numerical simulations such that nearly stable and strongly unstable solutions are found. Finally, some conclusions and discussions are given in Sec. VII.

II. N-FOLD DARBOUX TRANSFORMATION AND SOLUTIONS VIA THE DETERMINANTS

The dCNLS system (1) admits a Lax pair [31],

$$\begin{aligned} \Phi_x &= U\Phi, \quad U(\lambda,P) = \lambda J + P, \\ \Phi_t &= V\Phi, \\ V(\lambda,P,P_x) &= 2i\lambda^2\Sigma - 2\lambda P + i\Sigma(P^2 - P_x), \end{aligned} \tag{2}$$

where $\Phi = \Phi(x,t)$ is an eigenfunction, λ is a complex isospectral parameter, $J = -i\Sigma$, $\Sigma = \mathrm{diag}(-1,-1,1)$, and the potential matrix is

$$P = \begin{pmatrix} 0 & 0 & p \\ 0 & 0 & q \\ p^* & q^* & 0 \end{pmatrix},$$

where the star denotes the complex conjugation. The compatibility condition of the Lax pair (2) just generates the dCNLS equations (1). Inspired by the idea in [40,41], we can verify that system (1) admits the following DT.

Theorem 1. Let Φ_1 be a column vector solution for the Lax pair (2) with the initial potential function P and $\lambda = \lambda_1$; then the unified Darboux transformation of system (1) is given by

$$P[1] = P + [G,J], \tag{3}$$

where $G = \frac{(\lambda_1^* - \lambda_1)y_1 y_1^\dagger \Sigma}{y_1^\dagger \Sigma y_1}$, with $y_1 = \nu_1(x,t,\lambda)\Phi_1, \nu_1(x,t,\lambda) \neq 0$ being an arbitrarily complex function, and $\dagger$ representing the conjugate transpose.

Similarly, we also find the N-fold Darboux transformation of the dCNLS equation (1).

Theorem 2. Suppose Φ_j's are solutions of the Lax pair (2) with the initial solution (p,q) and distinct spectral parameters $\lambda = \lambda_j$, $(j = 1,2,\ldots,N)$ and $y_j = \nu_j\Phi_j$, where $\nu_j = \nu_j(x,t,\lambda_j)$ is some function of x and t; then the N-fold DT of system (1) is given by

$$p[N] = p - 2i\frac{\begin{vmatrix} \hat{M} & Y_3^\dagger \\ Y_1 & 0 \end{vmatrix}}{|\hat{M}|}, \quad q[N] = q - 2i\frac{\begin{vmatrix} \hat{M} & Y_3^\dagger \\ Y_2 & 0 \end{vmatrix}}{|\hat{M}|}, \tag{4}$$

where the Darboux matrix $T = I - Y\hat{M}^{-1}(\lambda I - S)^{-1}Y^\dagger\Sigma$, $S = \mathrm{diag}(\lambda_1^*,\ldots,\lambda_N^*)$, $\hat{M} = [y_i^\dagger\Sigma y_i/(\lambda_j - \lambda_i^*)]_{N\times N}$, y_j is the jth column of Y, and Y_j is the jth row of Y.

Particularly, if we choose the plane-wave seed solution (6), $\nu_j = e^{-i[\lambda_j x + 2(c_1^2 + c_2^2 - \lambda_j^2)t]}$,

$$y_j = \nu_j\Phi_j = K\begin{pmatrix} \Phi_j \\ \psi_j \\ \phi_j \end{pmatrix}, \quad \begin{pmatrix} \Phi_j \\ \psi_j \\ \phi_j \end{pmatrix} = \nu_j\hat{M}Nl_j,$$
$$j = 1,2,\ldots,N,$$

where $K, \hat{M}, N$ are given in Sec. III, l_j is column vector, then we can reduce DT (4) to the form

$$p[N] = c_1\frac{\left|\frac{\hat{M}}{2i} + \phi^\dagger\Phi\right|}{\left|\frac{\hat{M}}{2i}\right|}e^{i\theta_1}, \quad q[N] = c_2\frac{\left|\frac{\hat{M}}{2i} + \phi^\dagger\psi\right|}{\left|\frac{\hat{M}}{2i}\right|}e^{i\theta_2}, \tag{5}$$

where $\Phi = (\Phi_1,\ldots,\Phi_N)$, $\psi = (\psi_1,\ldots,\psi_N)$, and $\phi = (\phi_1,\ldots,\phi_N)$.

For the given initial solution (p,q), one can obtain the exact solutions of system (1) in terms of the above-obtained DT. In this paper, we restrict $\mathrm{Im}(\lambda_1) \geqslant 0$.

III. LOCALIZED WAVE SOLUTIONS FOR $\mathrm{Im}(\lambda_1) > 0$

We now begin with the "seed" solution of system (1) in the form of plane waves,

$$\begin{aligned} p(x,t) &= c_1 e^{i\theta_1}, \quad q(x,t) = c_2 e^{i\theta_2}, \\ \theta_j(x,t) &= a_j x - \left[a_j^2 + 2\left(c_1^2 + c_2^2\right)\right]t \quad (j = 1,2), \end{aligned} \tag{6}$$

to obtain localized solutions of system (1) by using the above-obtained DT, where $c_{1,2}$ are amplitude, $a_{1,2}$ are real wave numbers, the phase velocity is $a_j + 2(c_1^2 + c_2^2)/a_j$, and the group velocity is $2a_j$. The key and hard problem in the DT is how to find the proper eigenfunction Φ of the Lax pair (2).

The Lax pair (2) with the seed solution (6) and $\lambda = \lambda_1$ is a linear system with variable coefficients for Φ, which may be difficult to be solved directly. Following the idea [19], we can convert the Lax system into one with constant coefficients,

$$\begin{aligned} \Psi_{1x} &= -iU_0\Psi_1, \\ \Psi_{1t} &= i\left[U_0^2 + 2\lambda_1 U_0 + \left(2c_1^2 + 2c_2^2 - \lambda_1^2\right)I\right]\Psi_1, \end{aligned} \tag{7}$$

by a gauge transformation $\Phi_1 = K\Psi_1$, where

$$U_0 = \begin{pmatrix} a_1 - \lambda_1 & 0 & ic_1 \\ 0 & a_2 - \lambda_1 & ic_2 \\ ic_1 & ic_2 & \lambda_1 \end{pmatrix},$$

$$K = \begin{pmatrix} e^{i\theta_1} & & \\ & e^{i\theta_2} & \\ & & 1 \end{pmatrix}.$$

In the following we will discuss the solutions of the Lax Eq. (7) for two cases.

A. For the case $a_1 = a_2$

We further make the matrix transformation for Eq. (7),

$$\Psi_1 = M\Omega_1, \quad M = \begin{pmatrix} \frac{ic_1}{\chi - a_1} & \frac{ic_1}{\mu - a_1} & -c_2 \\ \frac{ic_2}{\chi - a_1} & \frac{ic_2}{\mu - a_1} & c_1 \\ 1 & 1 & 0 \end{pmatrix}, \tag{8}$$

where χ and μ are two distinct roots of the quadratic equation

$$x^2 - (a_1 + 2\lambda_1)x + 2a_1\lambda_1 + c_1^2 + c_2^2 = 0; \tag{9}$$

then Eq. (7) reduces to the Lax system with the eigenmatrices being the diagonal matrices

$$\begin{aligned} \Omega_{1x} &= -iK_0\Omega_1, \\ \Omega_{1t} &= i\left[K_0^2 + 2\lambda_1 K_0 + \left(2c_1^2 + 2c_2^2 - \lambda_1^2\right)I\right]\Omega_1, \end{aligned} \tag{10}$$

where $K_0 = M^{-1}U_0M = \mathrm{diag}(\chi - \lambda_1, \mu - \lambda_1, a_1 - \lambda_1)$, with $\chi \neq \mu$. The Lax system (10) can easily be solved to get its solutions $N = \mathrm{diag}(e^{-i\xi(\chi)}, e^{-i\xi(\mu)}, e^{-i\xi(a_1)})$, with $\xi(z) = (z - \lambda_1)x - [z^2 + 2(c_1^2 + c_2^2 - \lambda_1^2)]t$.

Thus, the fundamental solution of system (2) can be found as $\Phi_1 = KMN$.

Lemma 1 [42]. Let A be an $n \times n$ Hermitian matrix and the leading principal minor of order j be not zero, denoted by D_i. Then A and $\mathrm{diag}(D_1, \frac{D_2}{D_1}, \ldots, \frac{D_n}{D_{n-1}})$ are congruent.

Proof. When $n = 1$, the Lemma holds. Suppose any $(n-1) \times (n-1)$ Hermitian matrix A has the conclusion. In the following, we show that the $n \times n$ matrix also has the same conclusion. The $n \times n$ matrix A can be represented as $A = \begin{pmatrix} A_{n-1} & \alpha_{n-1} \\ \alpha_{n-1}^\dagger & a_{n,n} \end{pmatrix}$, where A_{n-1} is the $(n-1) \times (n-1)$ Hermitian matrix and α_{n-1} is a $n-1$ dimensional column vector. $a_{n,n}$ is a scalar value. By the assumption, there exists an $(n-1) \times (n-1)$ invertible matrix S_{n-1} satisfying $S_{n-1}^\dagger A_{n-1} S_{n-1} = \Lambda_{n-1}$, where $\Lambda_{n-1} = \mathrm{diag}(D_1, \frac{D_2}{D_1}, \ldots, \frac{D_{n-1}}{D_{n-2}})$. Let $S_n = \begin{pmatrix} S_{n-1} & -S_{n-1}\Lambda_{n-1}^{-1}S_{n-1}^\dagger\alpha_{n-1} \\ 0 & 1 \end{pmatrix}$, then $S_n^\dagger A S_n = \begin{pmatrix} \Lambda_{n-1} & 0 \\ 0 & b_n \end{pmatrix}$, where $b_n = 1 - \alpha_{n-1}^\dagger S_{n-1}\Lambda_{n-1}^{-1} S_{n-1}^\dagger\alpha_{n-1}$. Taking the determination, we can obtain $b_n = |\det S_n|^2 \frac{D_n}{D_{n-1}}$. Thus, A and $\mathrm{diag}(D_1, \frac{D_2}{D_1}, \ldots, \frac{D_n}{D_{n-1}})$ are congruent. This completes the proof of the lemma. ■

Notice that Σ is either a positive-definite or a negative-definite matrix, so $y_1^\dagger \Sigma y_1$ may be zero for some y_1. We will consider how to choose y_1 to make sure $y_1^\dagger \Sigma y_1 \neq 0$. Let l be a nonzero vector $l = (l_1, l_2, l_3)^T$ and $\nu_1 = e^{-i[\lambda x + 2(c_1^2 + c_2^2 - \lambda^2)t]}$. Then we choose y_1 in the form $y_1 = \nu_1\Phi_1 l = \nu_1 KMNl$ such that we have

$$y_1^\dagger \Sigma y_1 = (\nu_1\Phi_1 l)^\dagger \Sigma (\nu_1\Phi_1 l) = (\nu_1 Nl)^\dagger (M^\dagger \Sigma M)(\nu_1 Nl),$$

where

$$M^\dagger \Sigma M = \begin{pmatrix} \frac{2(\lambda_1^* - \lambda_1)}{\chi^* - \chi} & \frac{2(\lambda_1^* - \lambda_1)}{\chi^* - \mu} & 0 \\ \frac{2(\lambda_1^* - \lambda_1)}{\mu^* - \chi} & \frac{2(\lambda_1^* - \lambda_1)}{\mu^* - \mu} & 0 \\ 0 & 0 & -\left(c_1^2 + c_2^2\right) \end{pmatrix},$$

Thus, $y_1^\dagger \Sigma y_1$ is a complex quadratic form about matrix $M^\dagger \Sigma M$. Thus, by Lemma 1, $M^\dagger \Sigma M$ and diag $[\mathrm{Im}(\chi), \mathrm{Im}(\mu), -1]$ are congruent. Moreover, $\mathrm{Im}(\chi)\mathrm{Im}(\mu) < 0$. Without loss of generality, we assume $\mathrm{Im}(\chi) < 0, \mathrm{Im}(\mu) > 0$; thus, when $l_1 l_3 \neq 0, l_2 = 0$, we can obtain $y_1^\dagger \Sigma y_1 \neq 0$. If we take $l_1 = 1, l_2 = 0, l_3 = [-\frac{2\mathrm{Im}(\lambda_1)}{\mathrm{Im}(\chi)(c_1^2 + c_2^2)}]^{1/2}$, then we can obtain $y_1^\dagger \Sigma y_1 = \frac{2(\lambda_1^* - \lambda_1)}{\chi^* - \chi} e^{A_1}$, where $A_1 = 2\mathrm{Im}(\chi)[x - 2\mathrm{Re}(\chi)t]$.

Finally, it follows from Theorem 1 that we can obtain the solutions of system (1),

$$\begin{aligned} p[1] &= c_1 e^{i\theta_1}\left(\frac{C_1 - 1}{2}\tanh\frac{A_1}{2} + \frac{c_2 D_1}{c_1} \right. \\ &\quad \left. \times \mathrm{sech}\frac{A_1}{2} e^{iB_1} + \frac{C_1 + 1}{2}\right), \\ q[1] &= c_2 e^{i\theta_2}\left(\frac{C_1 - 1}{2}\tanh\frac{A_1}{2} - \frac{c_1 D_1}{c_2} \right. \\ &\quad \left. \times \mathrm{sech}\frac{A_1}{2} e^{iB_1} + \frac{C_1 + 1}{2}\right), \end{aligned} \tag{11}$$

where

$$\begin{aligned} C_1 &= \frac{\chi^* - a_1}{\chi - a_1}, \quad D_1 = \left[\frac{-2\mathrm{Im}(\lambda_1)\mathrm{Im}(\chi)}{c_1^2 + c_2^2}\right]^{1/2}, \\ B_1 &= [\mathrm{Re}(\chi) - a_1]x + \left[a_1^2 - \mathrm{Re}(\chi^2)\right]t + \frac{3}{2}\pi. \end{aligned}$$

By choosing special parameters, we can obtain the distinct wave structures of solutions (11) including the time-periodic breather solutions (see Fig. 1 for $c_{1,2} \neq 0$), which are also called temporal cavity solitons [43,44], and dark-bright solitons (see Fig. 2 for $c_2 = 0$); that is, the amplitudes $c_{1,2}$ of the seed solutions can modulate the wave structures. When $c_{1,2} \neq 0$, the two components p and q of the seed solution are both nonzero plane waves, which excites the new breather solutions, but when $c_1 \neq 0, c_2 = 0$ or $c_1 = 0, c_2 \neq 0$,

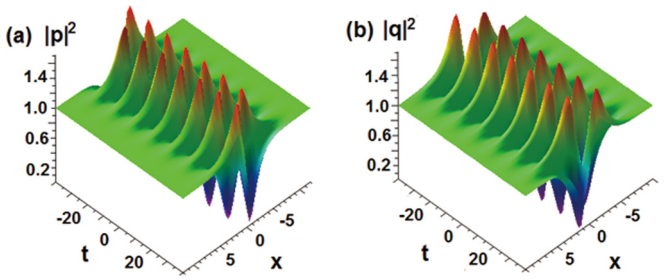

FIG. 1. The time-periodic breather solutions (11) with parameters $a_{1,2} = 0$, $c_{1,2} = 1$, $\lambda_1 = i$, $\chi = (1 - \sqrt{3})i$. (a) $|p|^2$; (b) $|q|^2$.

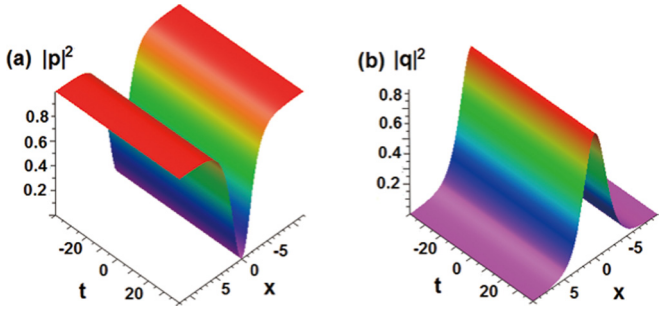

FIG. 2. Dark-bright solitons (11) with parameters $a_{1,2} = c_2 = 0$, $c_1 = 1$, $\lambda_1 = i$, $\chi = (1 - \sqrt{2})i$. (a) Dark soliton ($|p|^2$); (b) bright soliton ($|q|^2$).

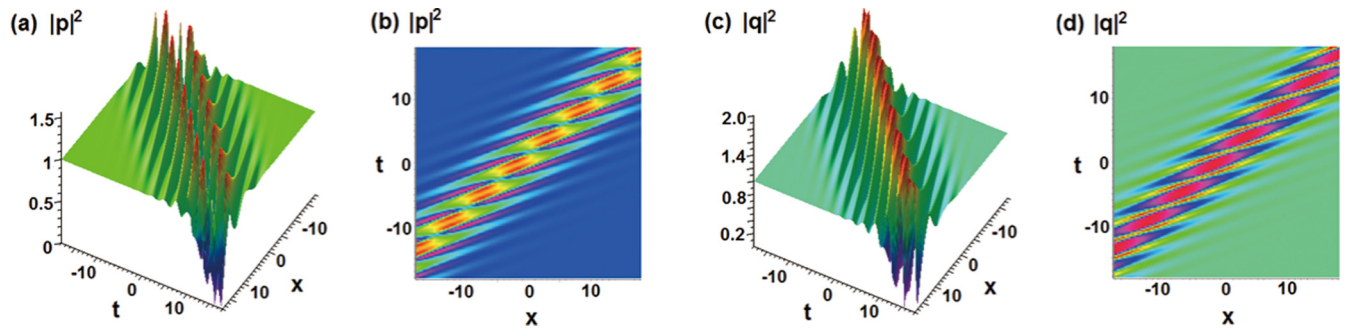

FIG. 3. Breather solutions (15): (a),(b) $|p|^2$; (c),(d) $|q|^2$; with parameters $a_1 = 4$, $a_2 = 0$, $c_{1,2} = 2$, $\lambda = i/2$, $l_{1,2} = 1$.

the two components p and q of the seed solution reduce to the case that one is a zero solution and another is a nonzero plane solution, which generates the dark-bright (or dark-bright) soliton solutions. It should be pointed out that the obtained breather solitons are of the potential significance for applications in many fields such as nonlinear optics, hydrodynamics, plasma physics, and superconductivity (see, e.g., [45,46] and references therein).

B. For the case $a_1 \neq a_2$

For the case $a_2 \neq a_1$, we have the matrix decomposition $M_1^{-1} U_0 M_1 = K_1$ with

$$K_1 = \mathrm{diag}(\chi - \lambda_1, \mu - \lambda_1, \nu - \lambda_1), \quad M_1 = \begin{pmatrix} \frac{ic_1}{\chi - a_1} & \frac{ic_1}{\mu - a_1} & \frac{ic_1}{\nu - a_1} \\ \frac{ic_2}{\chi - a_2} & \frac{ic_2}{\mu - a_2} & \frac{ic_2}{\nu - a_2} \\ 1 & 1 & 1 \end{pmatrix}, \tag{12}$$

where χ, μ, and ν are three different roots of the following cubic equation:

$$x^3 - (a_1 + a_2 + 2\lambda_1)x^2 + \left[a_1 a_2 + 2(a_1 + a_2)\lambda_1 + c_1^2 + c_2^2\right]x - (2a_1 a_2 \lambda_1 + a_1 c_2^2 + a_2 c_1^2) = 0. \tag{13}$$

Thus, the fundamental solution of system (2) can be found as $\Phi_1 = KMN$, where $N = \mathrm{diag}(e^{-i\xi(\chi)}, e^{-i\xi(\mu)}, e^{-i\xi(\nu)})$, with $\xi(z) = (z - \lambda_1)x - [z^2 + 2(c_1^2 + c_2^2 - \lambda_1^2)]t$.

It follows from the matrix

$$M_1^{\dagger} \Sigma M_1 = \begin{pmatrix} \frac{2(\lambda_1^* - \lambda_1)}{\chi^* - \chi} & \frac{2(\lambda_1^* - \lambda_1)}{\chi^* - \mu} & \frac{2(\lambda_1^* - \lambda_1)}{\chi^* - \nu} \\ \frac{2(\lambda_1^* - \lambda_1)}{\mu^* - \chi} & \frac{2(\lambda_1^* - \lambda_1)}{\mu^* - \mu} & \frac{2(\lambda_1^* - \lambda_1)}{\mu^* - \nu} \\ \frac{2(\lambda_1^* - \lambda_1)}{\nu^* - \chi} & \frac{2(\lambda_1^* - \lambda_1)}{\nu^* - \mu} & \frac{2(\lambda_1^* - \lambda_1)}{\nu^* - \nu} \end{pmatrix}$$

that we can find that $M_1^{\dagger} \Sigma M_1$ and $\mathrm{diag}[\mathrm{Im}(\chi), \mathrm{Im}(\mu), \mathrm{Im}(\nu)]$ are congruent. Without loss of generality, let us assume $\mathrm{Im}(\chi) < 0$, $\mathrm{Im}(\mu) < 0$, $\mathrm{Im}(\nu) > 0$. Finally, we take

$$y_1 = DM_1(\nu_1 Nl) = D \begin{pmatrix} \frac{ic_1}{\chi - a_1} & \frac{ic_1}{\mu - a_1} & \frac{ic_1}{\nu - a_1} \\ \frac{ic_2}{\chi - a_2} & \frac{ic_2}{\mu - a_2} & \frac{ic_2}{\nu - a_2} \\ 1 & 1 & 1 \end{pmatrix} \begin{pmatrix} l_1 e^{-iB(\chi)} \\ l_2 e^{-iB(\mu)} \\ 0 \end{pmatrix}, \tag{14}$$

where $B(z) = zx - z^2 t$, $C = i[B(\chi) - B(\mu)]$.

Case 1. Breather solutions. It follows from Theorem 1 that we find another family of breather solutions

$$p[1] = c_1 e^{i\theta_1} \left[\frac{\frac{(\chi^* - a_1)|l_1|^2}{\chi - a_1} + \frac{(\mu^* - a_1)(\chi^* - \chi)|l_2|^2}{(\mu^* - \mu)(\mu - a_1)} e^{C + C^*} + \frac{(\mu^* - a_1)(\chi^* - \chi) l_1 l_2^*}{(\mu^* - \chi)(\chi - a_1)} e^{C^*} + \frac{(\chi^* - a_1)(\chi^* - \chi) l_1^* l_2}{(\chi^* - \mu)(\mu - a_1)} e^{C}}{|l_1|^2 + \frac{(\chi^* - \chi)|l_2|^2}{\mu^* - \mu} e^{C + C^*} + \frac{(\chi^* - \chi) l_1 l_2^*}{\mu^* - \chi} e^{C^*} + \frac{(\chi^* - \chi) l_1^* l_2}{\chi^* - \mu} e^{C}} \right], \tag{15a}$$

$$q[1] = c_2 e^{i\theta_2} \left[\frac{\frac{(\chi^* - a_2)|l_1|^2}{\chi - a_2} + \frac{(\mu^* - a_2)(\chi^* - \chi)|l_2|^2}{(\mu^* - \mu)(\mu - a_2)} e^{C + C^*} + \frac{(\mu^* - a_2)(\chi^* - \chi) l_1 l_2^*}{(\mu^* - \chi)(\chi - a_2)} e^{C^*} + \frac{(\chi^* - a_2)(\chi^* - \chi) l_1^* l_2}{(\chi^* - \mu)(\mu - a_2)} e^{C}}{|l_1|^2 + \frac{(\chi^* - \chi)|l_2|^2}{\mu^* - \mu} e^{C + C^*} + \frac{(\chi^* - \chi) l_1 l_2^*}{\mu^* - \chi} e^{C^*} + \frac{(\chi^* - \chi) l_1^* l_2}{\chi^* - \mu} e^{C}} \right], \tag{15b}$$

which are displayed in Fig. 3. Figure 3 implies that the breather solutions (15) of system (1) are periodic in both spatial and temporal directions, which can be called the spatial-temporal cavity solitons and differ from the above-mentioned breather solutions (11), whose main reason is that the wave numbers $a_{1,2}$ of the seed solutions for breather solutions (11) are the same (see Fig. 1 with $a_1 = a_2 = 0$), but the wave numbers $a_{1,2}$ of the seed solutions for breather solutions (15) are distinct (see Fig. 3 with $a_1 = 4$, $a_2 = 0$).

Case 2. Rogue wave solutions. To obtain rogue wave solutions from the breather solutions (15), we choose $|l_1|^2 + |l_2|^2 + 2\mathrm{Re}(l_1 l_2^*) = 0$ and consider the limit process (as $\mu \to \chi$) such that the new vector rogue wave solutions of system (1) can be derived as

$$p[1] = c_1 \left[1 - \frac{2ir}{\chi - a_1} \frac{(x - 2st)^2 + 4r^2 t^2 - \frac{i}{\chi - a_1}(x - 2st + 2irt)}{\left(x - 2st - \frac{1}{2r}\right)^2 + 4r^2 t^2 + \frac{1}{4r^2}} \right] e^{i\theta_1},$$
$$q[1] = c_2 \left[1 - \frac{2ir}{\chi - a_2} \frac{(x - 2st)^2 + 4r^2 t^2 - \frac{i}{\chi - a_2}(x - 2st + 2irt)}{\left(x - 2st - \frac{1}{2r}\right)^2 + 4r^2 t^2 + \frac{1}{4r^2}} \right] e^{i\theta_2}, \tag{16}$$

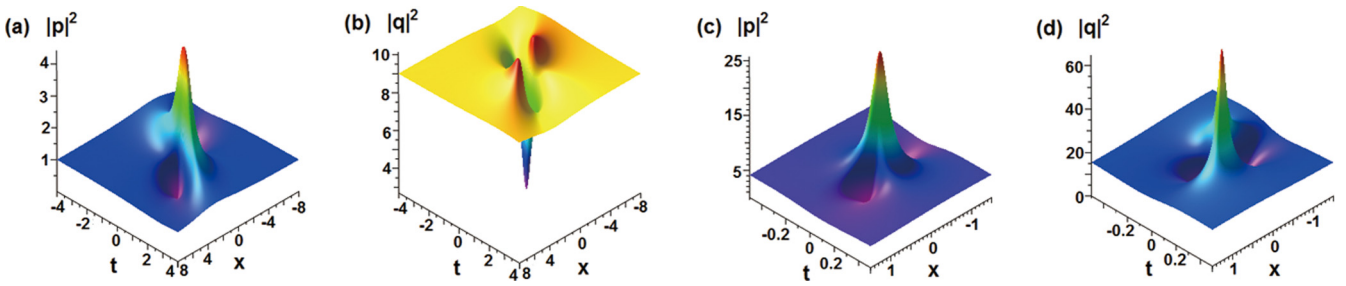

FIG. 4. (a) Bright and (b) dark rogue waves with parameters $a_1 = -a_2 = c_1 = 1$, $c_2 = 3$, $\lambda = 2.369\,536\,229 + 1.197\,202\,880i$, $\chi = 0.677\,924\,890\,0 - 0.600\,014\,1248i$. (c) Bright and bright rogue waves with parameter $a_1 = -a_2 = 1$, $c_1 = 2$, $c_2 = 4$, $\lambda = 1.421\,593\,632 + 2.562\,931\,182i$, $\chi = 0.225\,980\,808\,4 - 2.145\,543\,790i$.

where $s = \mathrm{Re}(\chi)$ and $r = \mathrm{Im}(\chi)$, which exhibit the distinct types of RW structures of system (1) including dark-dark, bright-bright, bright-dark, dark-four-petals RW solutions (see Figs. 4, 5, and 6). Particularly, there are two maximum and two minimum points for novel RWs in Figs. 5(c) and 5(d) and Fig. 6(b), which differ from the usual RW solutions. Notice that our results are of more new wave structures than the known ones [21]. Similar to Ref. [47,48], these obtained distinct types of rogue wave solutions may be active modulation for the stimulated supercontinuum generation.

IV. LOCALIZED WAVE SOLUTIONS FOR $\mathrm{Im}(\lambda_1) = 0$

When λ_1 is a real number, we can obtain the dark-dark solitons according to the above-mentioned Darboux transformation. We choose

$$y_1 = D\begin{pmatrix} \frac{ic_1}{\chi-a_1} & \frac{ic_1}{\chi^*-a_1} \\ \frac{ic_2}{\chi-a_2} & \frac{ic_2}{\chi^*-a_2} \\ 1 & 1 \end{pmatrix}\begin{pmatrix} e^{-iB} \\ \alpha(\lambda_1^*-\lambda_1)e^{-iB^*} \end{pmatrix} \tag{17}$$

such that we can obtain the dark-dark solitons of system (1),

$$\begin{aligned} p[1] &= \frac{c_1}{2}\left[1 + \frac{\chi^*-a_1}{\chi-a_1} - \frac{\chi-\chi^*}{\chi-a_1}\tanh(X)\right]e^{i\theta_1}, \\ q[1] &= \frac{c_2}{2}\left[1 + \frac{\chi^*-a_2}{\chi-a_2} - \frac{\chi-\chi^*}{\chi-a_2}\tanh(X)\right]e^{i\theta_2}, \end{aligned} \tag{18}$$

where

$$X = \mathrm{Im}(\chi)[x - 2\mathrm{Re}(\chi)t] - \frac{1}{2}\ln\beta,$$
$$\beta = 2\mathrm{Im}(\chi)\mathrm{Im}\left\{\left[1 - \frac{1}{(\chi^*-a_1)^2} - \frac{1}{(\chi^*-a_2)^2}\right]\alpha\right\} > 0.$$

Figure 7 displays the usual dark-dark solitons of system (1) for the distinct parameters.

V. INTERACTIONS OF LOCALIZED WAVE SOLUTIONS

In the following we will investigate the interactions of distinct types of solutions.

A. Interactions with $N = 2$ and $a_2 \neq a_1$

Case 1. Interactions of dark-dark and breather-breather solutions. For this case, we choose

$$\begin{aligned} \begin{pmatrix} \Phi_1 \\ \psi_1 \\ \phi_1 \end{pmatrix} &= \begin{pmatrix} \frac{i}{\chi_1-a_1} & \frac{i}{\mu_1-a_1} \\ \frac{i}{\chi_1-a_2} & \frac{i}{\mu_1-a_2} \\ 1 & 1 \end{pmatrix}\begin{pmatrix} e^{-iA_1} \\ e^{-iB_1} \end{pmatrix}, \\ \begin{pmatrix} \Phi_2 \\ \psi_2 \\ \phi_2 \end{pmatrix} &= \begin{pmatrix} \frac{i}{\chi_2-a_1} & \frac{i}{\chi_2^*-a_1} \\ \frac{i}{\chi_2-a_2} & \frac{i}{\chi_2^*-a_2} \\ 1 & 1 \end{pmatrix}\begin{pmatrix} e^{-iA_2} \\ \alpha(\lambda_2^*-\lambda_2)e^{-iA_2^*} \end{pmatrix}, \end{aligned} \tag{19}$$

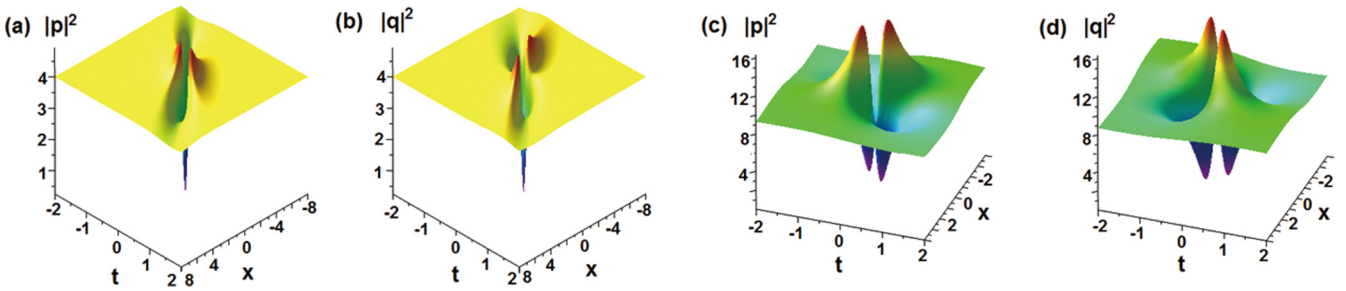

FIG. 5. (a) Dark and (b) dark rogue waves with parameters $a_1 = 4$, $a_2 = 0$, $c_1 = c_2 = 2$, $\lambda = 1 + \frac{1}{2}i\sqrt{-22 + 10\sqrt{5}}$, $\chi = -\frac{1}{2}i\sqrt{-22 + 10\sqrt{5}}\sqrt{5} - \frac{1}{2}i\sqrt{-22 + 10\sqrt{5}} + 2$. (c),(d) Four-petals rogue wave with parameters $a_1 = -a_2 = 1$, $c_1 = c_2 = 3$, $\lambda = 4.025\,178\,563i$, $\chi = 0.000\,000\,000\,0 - 0.903\,701\,720\,4i$.

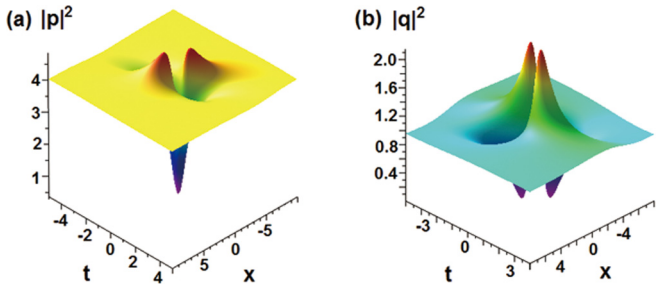

FIG. 6. (a) Dark rogue wave and (b) four-petals rogue wave with parameters $a_1 = -a_2 = c_2 = 1$, $c_1 = 2$, $\lambda = -0.991\,854\,667\,7 + 0.636\,002\,000\,8i$, $\chi = -0.399\,160\,590\,9 - 0.645\,847\,282\,8i$.

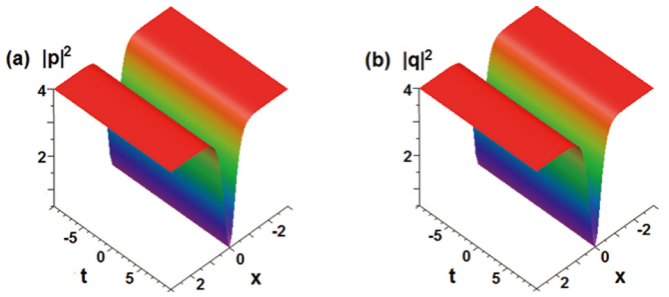

FIG. 7. Dark-dark solitons (18) with parameters $a_1 = 1$, $a_2 = -1$, $c_{1,2} = 2$, $\lambda_1 = \beta = 0$, $\chi = -i\sqrt{7}$. (a) $|p|^2$; (b) $|q|^2$.

where $A_j = \chi_j x - \chi_j^2 t$ $(j = 1,2)$, $B_1 = \mu_1 x - \mu_1^2 t$, and $\beta = 2\mathrm{Im}(\chi_2)\mathrm{Im}\{[1 - \frac{1}{(\chi_2^* - a_1)^2} - \frac{1}{(\chi_2^* - a_2)^2}]\alpha\} > 0$ for some α. we can obtain general formulas,

$$p[2] = c_1 \frac{D_1}{D} e^{i\theta_1}, \quad q[2] = c_2 \frac{D_2}{D} e^{i\theta_2}, \tag{20}$$

where

$$D = \frac{e^{2\mathrm{Re}(C_2)} + \beta}{4\mathrm{Im}(\chi_2)}\left[\frac{1}{\mathrm{Im}(\chi_1)} + \frac{e^{2\mathrm{Re}(C_1)}}{\mathrm{Im}(\mu_1)} - 4\mathrm{Im}\left(\frac{e^{C_1}}{\chi_1^* - \mu_1}\right)\right] + e^{2\mathrm{Re}(C_2)}\left|\frac{1}{\chi_1^* - \chi_2} + \frac{e^{C_1^*}}{\mu_1^* - \chi_2}\right|^2,$$

$$D_i = \frac{\frac{\chi_2^* - a_i}{\chi_2 - a_i} e^{2\mathrm{Re}(C_2)} + \beta}{2\mathrm{Im}(\chi_2)}\left[\frac{\chi_1^* - a_i}{\chi_1 - a_i}\frac{1}{2\mathrm{Im}(\chi_1)} + \frac{\mu_1^* - a_i}{\mu_1 - a_i}\frac{e^{2\mathrm{Re}(C_1)}}{2\mathrm{Im}(\mu_1)} - \frac{\mu_1^* - a_i}{\chi_1 - a_i}\frac{e^{C_1^*}}{\mu_1^* - \chi_1} - \frac{\chi_1^* - a_i}{\mu_1 - a_i}\frac{e^{C_1}}{\chi_1^* - \mu_1}\right] - e^{2\mathrm{Re}(C_2)}\left(\frac{\chi_1^* - a_i}{\chi_2 - a_i}\frac{1}{\chi_1^* - \chi_2} + \frac{\mu_1^* - a_i}{\chi_2 - a_i}\frac{e^{C_1^*}}{\mu_1^* - \chi_2}\right) \times \left(\frac{\chi_2^* - a_i}{\chi_1 - a_i}\frac{1}{\chi_2^* - \chi_1} + \frac{\chi_2^* - a_i}{\mu_1 - a_i}\frac{e^{C_1}}{\chi_2^* - \mu_1}\right),$$

and $C_1 = -i(\mu_1 - \chi_1)[x - (\mu_1 + \chi_1)t]$, $C_2 = -i\chi_2(x - \chi_2 t)$.

By choosing special parameters, we can obtain the distinct wave structures of solutions (20) including the parallel strong interactions of dark-dark and time-periodic breather-breather solutions (see Figs. 8 and 9), vertical strong interactions of dark-dark and space-periodic breather-breather solutions (see Fig. 10), the parallel weak interactions of dark-dark and time-periodic breather-breather solutions (see Fig. 11), and the cross strong interactions of dark-dark and (space, time)-periodic breather-breather solutions (see Fig. 12). It follows from Figs. 8–10) that for the fixed $a_1 = -a_2 = 1$, $c_{1,2} = 2$, $\lambda_2 = \beta = 1$, we change λ_1 such that (i) when $\lambda_1 = i, 1.5i$, Figs. 8 and 9 display the similar profiles except for the distinct temporal periods. Moreover, its period becomes bigger for the larger $|\lambda_1|$; (ii) when the imaginary part of λ_1 becomes larger, e.g., $\lambda_1 = 2i$, the parallel interactions (see Figs. 8 and 9) are changed into the vertical interactions (see Fig. 10), and the time-periodic profiles are also changed to the space-periodic one.

Case 2. Interactions of dark solitons and rogue wave solutions. Next, we analyze the interaction between dark-dark solitons and rogue wave solutions. We take the limit technique $\mu_1 \to \chi_1$ such that we can obtain solutions of system (1),

$$p[2] = c_1\left(\frac{D_1}{D}\right)e^{i\theta_1}, \quad q[2] = c_2\left(\frac{D_2}{D}\right)e^{i\theta_2}, \tag{21}$$

where

$$D = \frac{\beta + e^{2\mathrm{Re}(C_2)}}{4\mathrm{Im}(\chi_1)\mathrm{Im}(\chi_2)}\left\{|x - 2\chi_1 t|^2 - \frac{i\mathrm{Re}(x - 2\chi_1 t)}{\mathrm{Im}(\chi_1)} - \frac{1}{2[\mathrm{Im}(\chi_1)]^2}\right\} + \frac{e^{2\mathrm{Re}(C_2)}}{|\chi_1^* - \chi_2|^2}\left|i(x - 2\chi_1^* t) - \frac{1}{\chi_1^* - \chi_2}\right|^2,$$

$$D_i = F_i\left[\frac{\beta}{\chi_2^* - \chi_2} + \frac{(\chi_2^* - a_i)e^{2\mathrm{Re}(C_2)}}{(\chi_2 - a_i)(\chi_2^* - \chi_2)}\right] + \frac{(\chi_1^* - a_i)}{\chi_2 - a_i}\left[-\frac{1}{(\chi_1^* - a_i)(\chi_1^* - \chi_2)} + \frac{1}{(\chi_1^* - \chi_2)^2} - \frac{i(x - 2\chi_1^* t)}{\chi_1^* - \chi_2}\right] \times \frac{\chi_2^* - a_i}{\chi_1 - a_i}\left[-\frac{1}{(\chi_1 - a_i)(\chi_2^* - \chi_1)} + \frac{1}{(\chi_2^* - \chi_1)^2} - \frac{i(x - 2\chi_1 t)}{\chi_2^* - \chi_1}\right]e^{2\mathrm{Re}(C_2)},$$

$$F_i = \frac{\chi_1^* - a_i}{2(\chi_1 - a_i)\mathrm{Im}(\chi_1)}\left\{\frac{i\mathrm{Re}(x - 2\chi_1 t)}{\mathrm{Im}(\chi_1)} + \frac{1}{2[\mathrm{Im}(\chi_1)]^2} - |x - 2\chi_1 t|^2\right\} + \frac{1}{2\mathrm{Im}(\chi_1)(\chi_1^* - a_i)}\left[i(x - 2\chi_1 t) + i(x - 2\chi_1^* t)\frac{\chi_1^* - a_i}{\chi_1 - a_i} + \frac{1}{\mathrm{Im}(\chi_1)}\right],$$

and $C_2 = -i\chi_2(x - \chi_2 t)$.

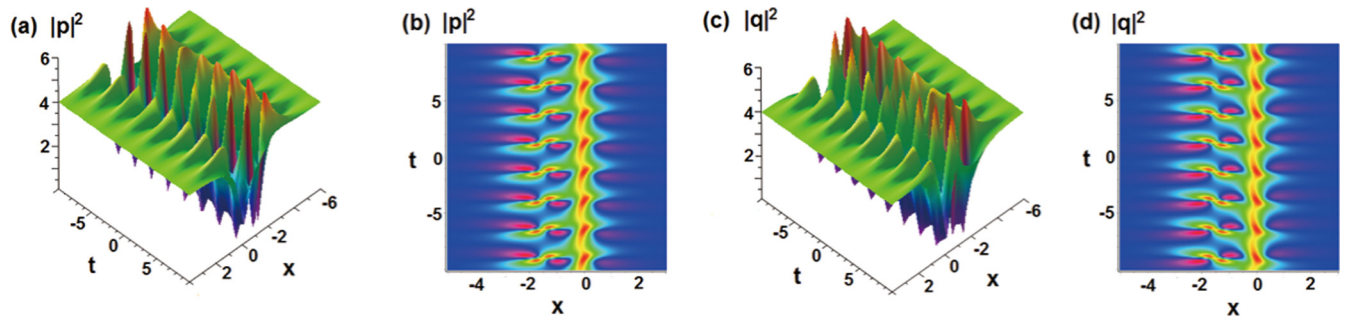

FIG. 8. Interactions of dark-dark and time-periodic breather-breather solutions with parameters $a_1 = -a_2 = 1$, $c_{1,2} = 2$, $\lambda_1 = i$, $\lambda_2 = \beta = 1$, $\chi_1 = -1.597\,735\,188\,118\,88i$, $\mu_1 = -0.319\,550\,804\,974\,658i$, $\chi_2 = -\sqrt{7}i$. (a), (b) $|p|^2$; (c), (d) $|q|^2$.

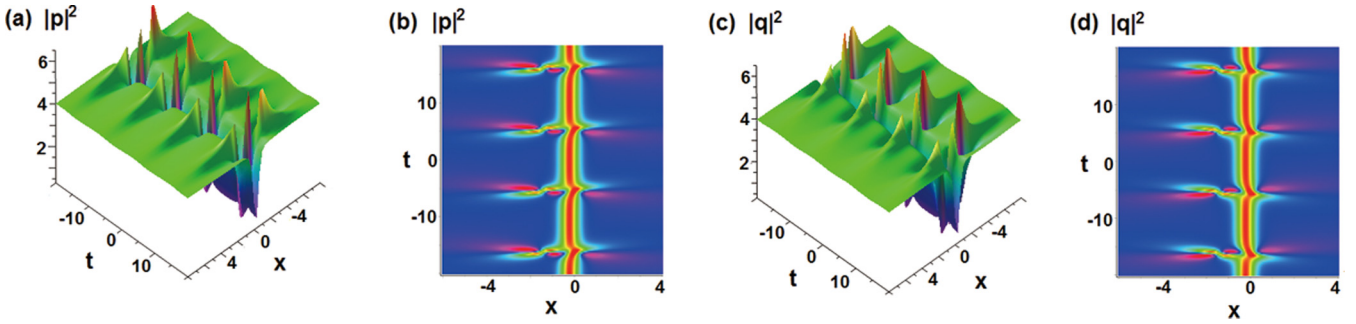

FIG. 9. Interactions of dark-dark and time-periodic breather-breather solutions with parameters $a_1 = -a_2 = 1$, $c_{1,2} = 2$, $\lambda_1 = 1.5i$, $\lambda_2 = \beta = 1$, $\chi_1 = -1.000\,000\,000\,0i$, $\mu_1 = -0.645\,751\,311\,1i$, $\chi_2 = -\sqrt{7}i$. (a), (b) $|p|^2$; (c), (d) $|q|^2$.

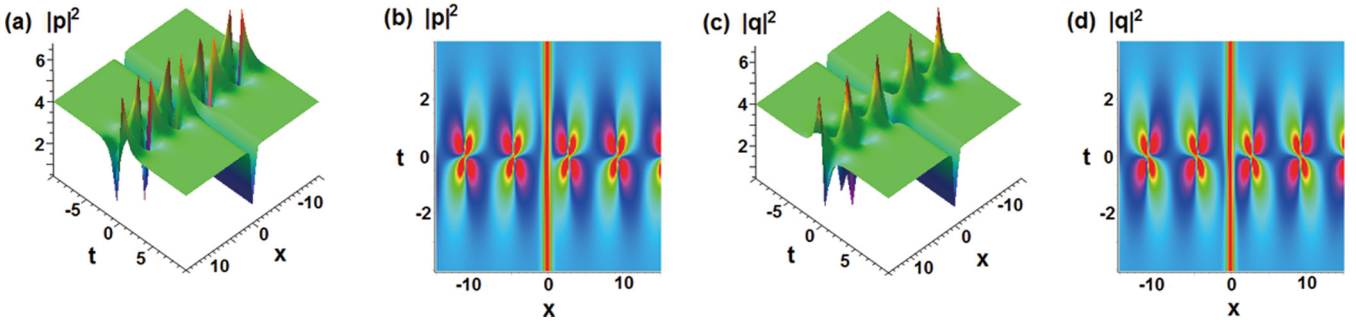

FIG. 10. Interactions of dark-dark and space-periodic breather-breather solutions with parameters $a_1 = -a_2 = 1$, $c_{1,2} = 2$, $\lambda_1 = 2i$, $\lambda_2 = \beta = 1$, $\chi_1 = -0.478\,389\,888\,327\,022 - 0.712\,979\,628\,930\,493i$, $\mu_1 = 0.478\,389\,888\,327\,022 - 0.712\,979\,628\,930\,493i$, $\chi_2 = -\sqrt{7}i$. (a), (b) $|p|^2$; (c), (d) $|q|^2$.

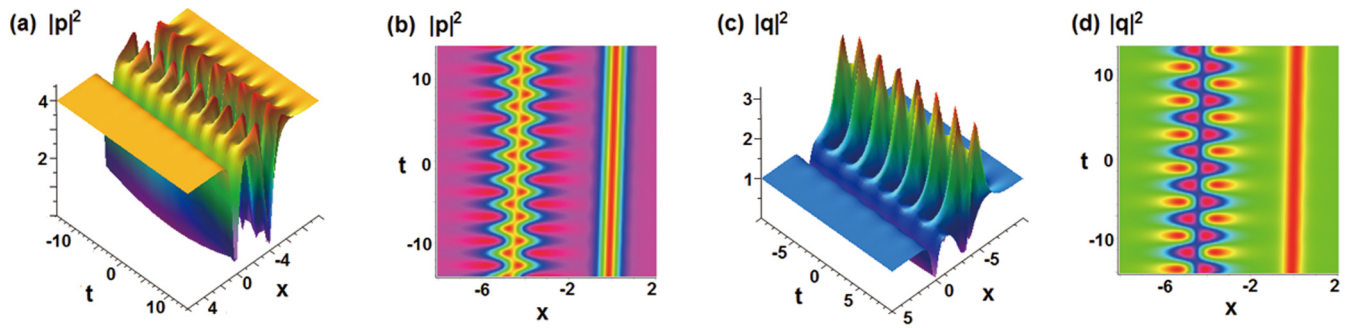

FIG. 11. Interactions of dark-dark and (space, time)-periodic breather-breather solutions with parameters $a_1 = \frac{1}{50}$, $a_2 = -\frac{1}{50}$, $c_1 = 2$, $c_2 = 1$, $\lambda_1 = i$, $\lambda_2 = 0$, $\chi_1 = 0.845\,107\,014\,6 - 1.449\,359\,273i$, $\mu_1 = -0.120\,015\,975\,2 - 0.102\,388\,198\,7i$, $\chi_2 = 0.600\,030\,719\,8 - 2.236\,002\,686i$, $\beta = 1$. (a), (b) $|p|^2$; (c), (d) $|q|^2$.

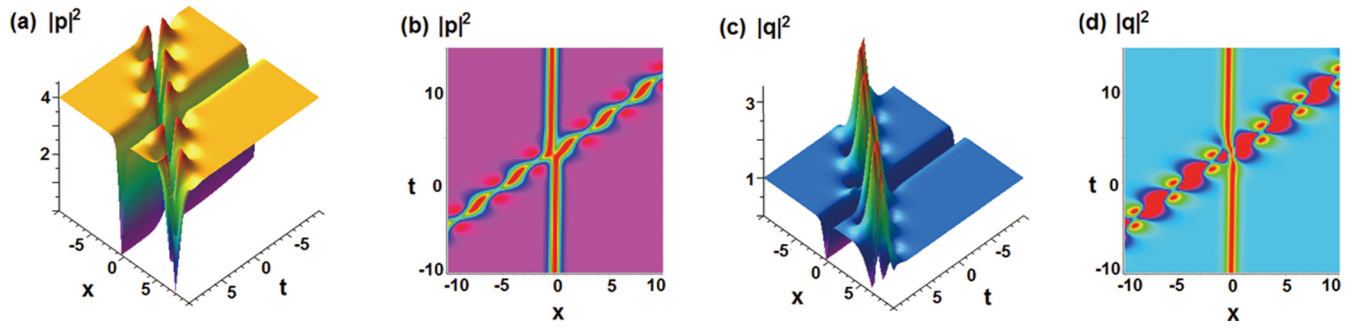

FIG. 12. Interactions of dark-dark and (space, time)-periodic breather-breather solutions with parameters $a_1 = \frac{1}{50}$, $a_2 = -\frac{1}{50}$, $c_1 = 2$, $c_2 = 1$, $\lambda_1 = 1 + i$, $\lambda_2 = 0$, $\chi_1 = 0.570\,266\,583\,5 - 1.280\,656\,011i$, $\mu_1 = -0.121\,029\,972\,3 - 0.100\,437\,747\,8i$, $\chi_2 = 0.600\,030\,719\,8 - 2.236\,002\,686i, \beta = 1$. (a), (b) $|p|^2$; (c), (d) $|q|^2$.

By choosing special parameters, we can find some distinct wave structures: strong interactions of dark-dark solitons and dark-dark rogue wave solutions (Fig. 13) and dark-dark solitons and bright-dark rogue wave solutions (Fig. 14). It follows from Fig. 13 that the interactions mainly focus on the dark solitons and the branches under the nonzero backgrounds of dark rogue waves; however, it follows from Fig. 14 that the interactions mainly focus on the dark solitons and the branches above the nonzero backgrounds of bright-dark rogue waves.

B. Interactions of localized waves for $N = 2$ and $a_1 = a_2$

For the special case $a_1 = a_2$, we choose special solutions

$$\begin{pmatrix}\Phi_1\\ \psi_1\\ \phi_1\end{pmatrix} = \begin{pmatrix}\frac{i}{\chi_1-a_1} & -d_1\\ \frac{i}{\chi_1-a_1} & d_2\\ 1 & 1\end{pmatrix}\begin{pmatrix}e^{-iA_1}\\ e^{-iB_1}\end{pmatrix},$$
$$\begin{pmatrix}\Phi_2\\ \psi_2\\ \phi_2\end{pmatrix} = \begin{pmatrix}\frac{i}{\chi_2-a_1} & \frac{i}{\chi_2^*-a_1}\\ \frac{i}{\chi_2-a_2} & \frac{i}{\chi_2^*-a_2}\\ 1 & 1\end{pmatrix}\begin{pmatrix}e^{-iA_2}\\ \alpha(\lambda_2^*-\lambda_2)e^{-iA_2^*}\end{pmatrix}, \quad (22)$$

where $A_j = \chi_j x - \chi_j^2 t\ (j = 1,2)$, $B_1 = a_1 x - a_1^2 t$, and $d_1 = \frac{c_2}{c_1}$, $d_2 = \frac{1}{d_1}$. As a result, we can obtain the solutions of system (1)

$$p[2] = c_1\frac{D_1}{D}e^{i\theta_1}, \quad q[2] = c_2\frac{D_2}{D}e^{i\theta_2}, \quad (23)$$

where

$$D = \frac{e^{2\mathrm{Re}(C_2)}+\beta}{\chi_2^*-\chi_2}\left[\frac{1}{\chi_1^*-\chi_1} - \frac{c_1^2+c_2^2}{2(\lambda_1^*-\lambda_1)}e^{2\mathrm{Re}(C_1)}\right] - \frac{e^{2\mathrm{Re}(C_2)}}{(\chi_1^*-\chi_2)(\chi_2^*-\chi_1)},$$
$$D_1 = \frac{\frac{\chi_2^*-a_1}{\chi_2-a_1}e^{2\mathrm{Re}(C_2)}+\beta}{\chi_2^*-\chi_2}\left[\frac{\chi_1^*-a_1}{\chi_1-a_1}\frac{1}{\chi_1^*-\chi_1} - \frac{c_1^2+c_2^2}{2(\lambda_1^*-\lambda_1)}e^{2\mathrm{Re}(C_1)} + id_1e^{c_1}\right] - \frac{\chi_1^*-a_1}{\chi_2-a_1}\frac{e^{2\mathrm{Re}(C_2)}}{\chi_1^*-\chi_2} \times\left(\frac{\chi_2^*-a_1}{\chi_1-a_1}\frac{1}{\chi_2^*-\chi_1}+id_1e^{C_1}\right),$$
$$D_2 = \frac{\frac{\chi_2^*-a_1}{\chi_2-a_1}e^{2\mathrm{Re}(C_2)}+\beta}{\chi_2^*-\chi_2}\left[\frac{\chi_1^*-a_1}{\chi_1-a_1}\frac{1}{\chi_1^*-\chi_1} - \frac{c_1^2+c_2^2}{2(\lambda_1^*-\lambda_1)}e^{2\mathrm{Re}(C_1)} - id_2e^{c_1}\right] - \frac{\chi_1^*-a_1}{\chi_2-a_1}\frac{e^{2\mathrm{Re}(C_2)}}{\chi_1^*-\chi_2} \times\left(\frac{\chi_2^*-a_1}{\chi_1-a_1}\frac{1}{\chi_2^*-\chi_1}-id_2e^{C_1}\right),$$

and $C_1 = i(\chi_1 - a_1)[x - (a_1 + \chi_1)t]$, $C_2 = -i\chi_2(x - \chi_2 t)$.

By choosing special parameters, we can obtain the pattern of interactions between temporal breather-breather solutions and dark-dark solitons (see Fig. 15). Figure 15 implies that the interactions are elastic and the interaction style for the component p begins with the suction part of the breather

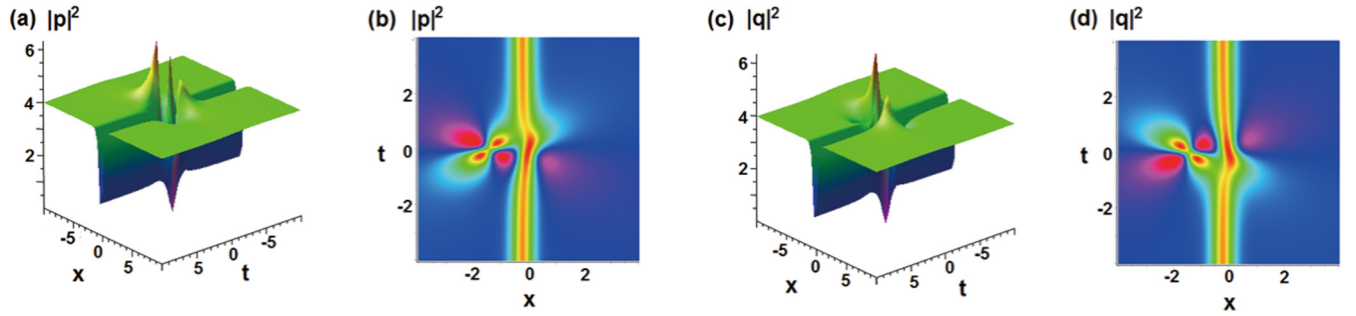

FIG. 13. Interactions of dark-dark solitons and dark-dark rogue-rogue wave solutions with parameters $a_1 = -a_2 = 1$, $c_{1,2} = 2$, $\beta = 1$, $\lambda_1 = \frac{1}{2}i\sqrt{16\sqrt{2}-13}$, $\lambda_2 = 0$, $\chi_1 = -\frac{2i}{7}\sqrt{16\sqrt{2}-13}\sqrt{2} + \frac{i}{7}\sqrt{16\sqrt{2}-13}$, $\chi_2 = -i\sqrt{7}$. (a), (b) $|p|^2$; (c), (d) $|q|^2$.

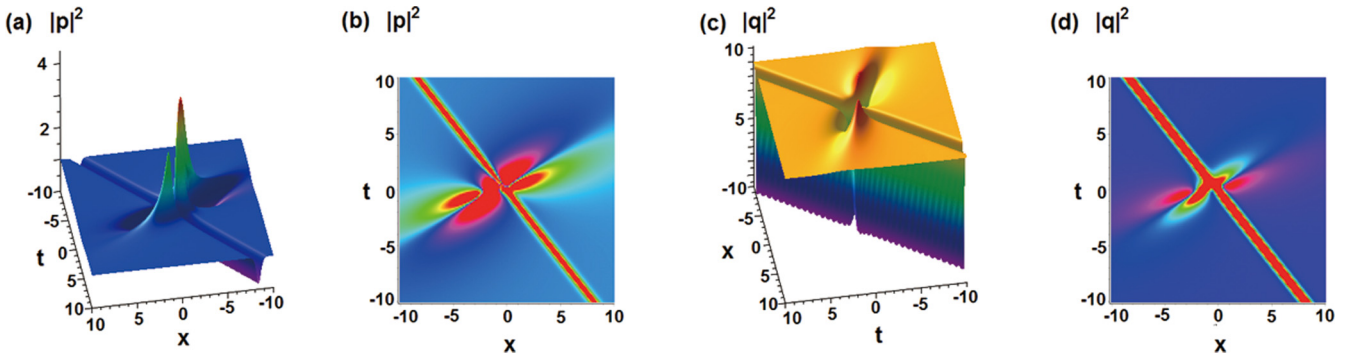

FIG. 14. Interactions of dark-dark solitons and bright-dark rogue wave solutions with parameters $a_1 = -a_2 = 1$, $\beta = c_1 = 1$, $c_2 = 3$, $\lambda_1 = 2.369\,536\,229 + 1.197\,202\,880i$, $\lambda_2 = 0$, $\chi_1 = 0.677\,924\,890\,0 - 0.600\,014\,124\,8i$, $\chi_2 = -0.413\,110\,434\,6 - 3.084\,149\,914i$. (a), (b) $|p|^2$; (c), (d) $|q|^2$.

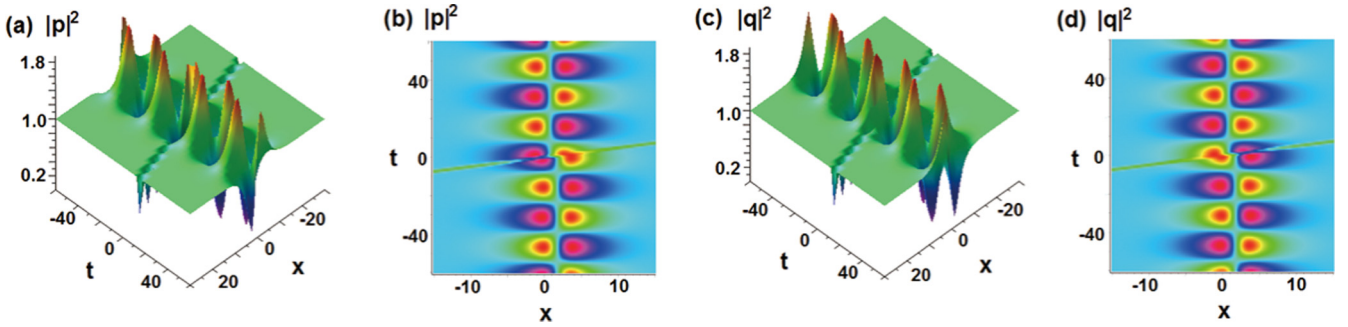

FIG. 15. Interaction of breather-breather and dark-dark solitons with parameters $a_{1,2} = 0$, $c_{1,2} = 1$, $\lambda_1 = 2i$, $\lambda_2 = \beta = 1$, $\chi_1 = (2 - \sqrt{6})i$, $\chi_2 = 1 - i$. (a), (b) $|p|^2$; (c), (d) $|q|^2$.

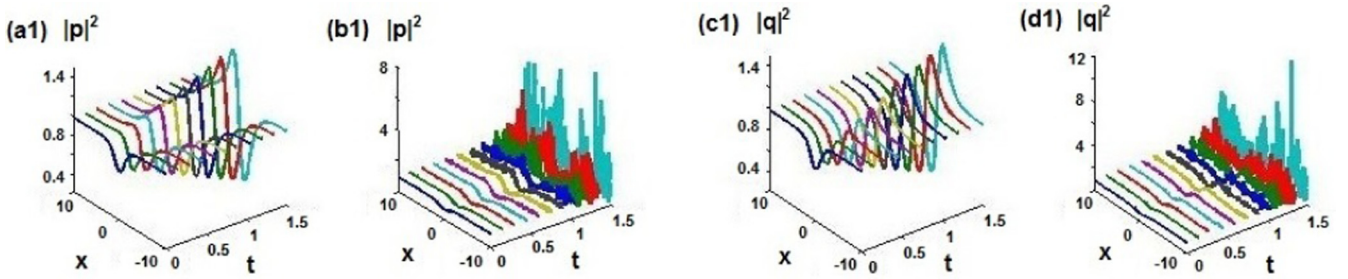

FIG. 16. Dynamical behaviors of time-periodic breather solutions (11) with parameters $a_{1,2} = 0$, $c_{1,2} = 1$, $\lambda_1 = i$, $\chi = (1 - \sqrt{3})i$ (see Fig. 1). (a1),(c1) Simulated evolution using breather solutions (11) as the initial conditions without a noise; (b1),(d1) the evolution initiated by the exact solution perturbed by weak random noise with amplitude 0.02.

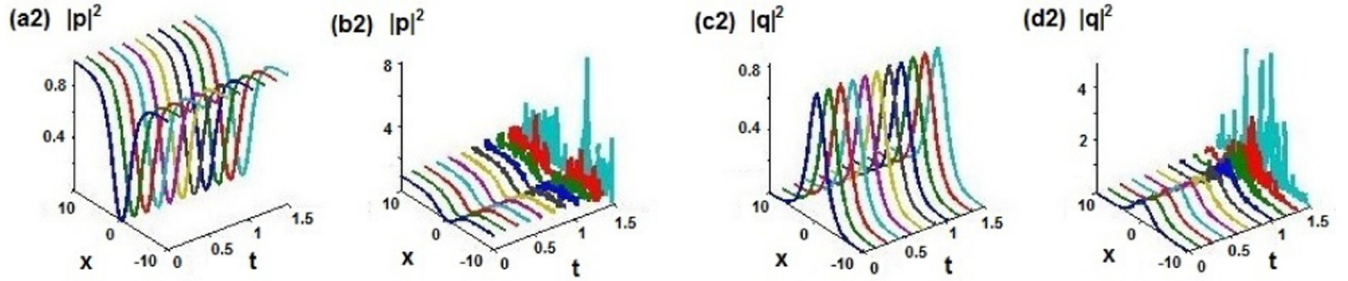

FIG. 17. Dynamical behaviors of dark-bright soliton solutions (11) with parameters $a_{1,2} = c_2 = 0$, $c_1 = 1$, $\lambda_1 = i$, $\chi = (1 - \sqrt{2})i$ (see Fig. 2). (a1),(c1) Simulated evolution using dark-bright soliton solutions (11) as the initial conditions without a noise; (b1),(d1) the evolution initiated by the dark-bright soliton solutions perturbed by weak random noise with amplitude 0.02.

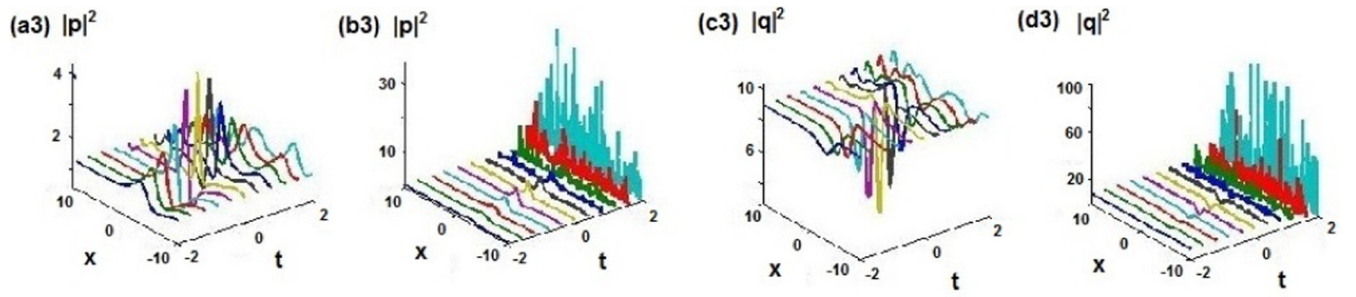

FIG. 18. Dynamical behaviors of bright-dark rogue wave solutions (16) with parameters $a_{1,2} = c_2 = 0$, $c_1 = 1$, $\lambda_1 = i$, $\chi = (1-\sqrt{2})i$ [see Figs. 4(a) and 4(b)]. (a1),(c1) Simulated evolution using bright-dark rogue wave solutions (16) as the initial conditions without a noise; (b1),(d1) the evolution initiated by the bright-dark rogue wave solutions perturbed by weak random noise with amplitude 0.02.

solution and then finishes with its calling part [see Figs. 15(a) and 15(b)]; however, the interaction style for the component q is opposite [see Figs. 15(c) and 15(d)]. The new pattern containing the dark soliton and temporal breather solution may excite the study of new soliton dynamics in the related nonlinear science such as nonlinear optics [1,2,45] and Bose-Einstein condensates [7].

VI. DYNAMICAL BEHAVIORS OF THE SOLUTIONS

To further exhibit the wave propagations of the above-found solutions, we here consider their dynamical behaviors by comparing them with their time evolution using them as the initial conditions with a small noise 2% in terms of numerical simulations.

Figures 16(a1) and 16(c1) illustrate the time evolutions of the temporal breather solutions (11) (see Fig. 1). Figures 16(b1) and 16(d1) exhibit the time evolution of temporal breather solutions (11) perturbated by a small noise 2% as the initial conditions. Figures 16(b1) and 16(d1) exhibit obviously strong instability for the simulated evolutions at about $t > 1$. This may happen due to the rapid changes of the amplitudes of the temporal breather solutions.

Figures 17(a2) and 17(c2) illustrate the time evolutions of the dark-bright soliton solutions (11), with $c_2 = 0$ (see Fig. 2). Figures 17(b1) and 17(d1) exhibit the time evolution of the dark-bright soliton (11) perturbated by a small noise 2% as the initial conditions. Figures 17(b1) and 17(d1) also display an obviously strong instability for the the simulated evolutions at about $t > 1$. This may happen due to the interaction of dark and bright solitons in this nonlinear system.

Figures 18(a3) and 18(c3) exhibit the stable wave evolutions of the bright-dark rogue wave solutions (16) in the absence of the initially added random noise [see Figs. 4(a) and 4(b)]. Figures 18(b1) and 18(d1) exhibit the time evolution of the bright-dark rogue wave solutions (16) perturbated by a small noise 2% as the initial conditions such that the simulated evolutions show obviously strong instability at about $t > 0.8$. This may happen due to the interaction of bight and dark rogue wave solutions in this nonlinear system.

Figures 19(a4) and 19(c4) display the stable wave evolutions of the bright-bright rogue wave solutions (16) in the absence of the initially added random noise [see Figs. 4(c) and 4(d)]. Figures 19(b4) and 19(d4) exhibit the time evolution of the bright-bright rogue wave solutions (16) perturbated by a small noise 2% as the initial conditions such that the simulated evolutions appear almost stable. This may happen due to the two components p and q possessing the similar bright rogue wave patterns in this nonlinear system.

VII. CONCLUSIONS AND DISCUSSIONS

We have used the matrix analysis method to avoid singularity and derived some newly localized wave solutions for the defocusing coupled nonlinear Schrödinger equation (1) by using the generalized N-fold Darboux transformation. A variety of obtained patterns contain the dark-dark solitons, bright-dark solitons, breather-breather solutions, and distinct types of vector rogue wave solutions (e.g., dark-dark, bright-bright, bright-dark, dark-pair, pair-pair rogue waves solutions). We also find the general N-fold Darboux transformation to generate the various of interactions between distinct types of

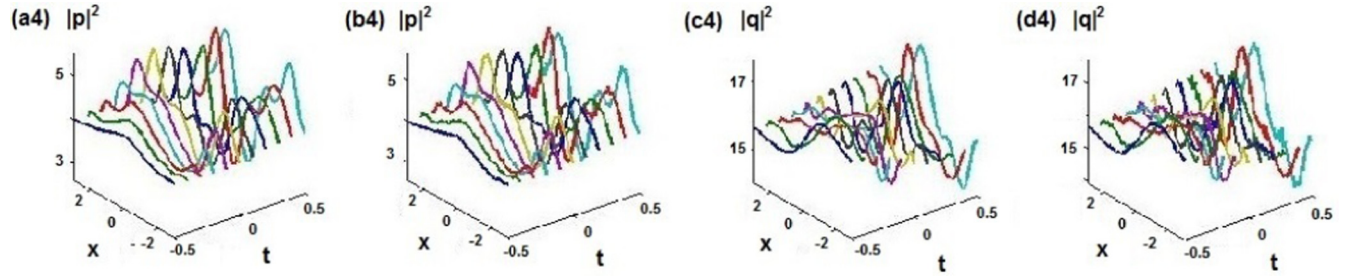

FIG. 19. Dynamical behaviors of bright-bright rogue wave solutions (16) with parameters $a_{1,2} = c_2 = 0, c_1 = 1, \lambda_1 = i, \chi = (1-\sqrt{2})i$ [see Figs. 4(c) and 4(d)]. (a1),(c1) Simulated evolution using bright-bright rogue wave solutions (16) as the initial conditions without a noise; (b1),(d1) the evolution initiated by the bright-bright rogue wave solutions perturbed by weak random noise with amplitude 0.02.

patterns (e.g., dark solitons and breather solutions, as well as dark solitons and RW solutions). Moreover, we also analyze the parameter modulation for these solutions. Finally, for some respective waves, we numerically illustrate their dynamical behaviors such that we find all considered waves have the stable wave propagations without a noise, and the most considered waves have the strongly unstable behaviors under the role of a small noise 2% except that the bright-bright rogue waves display the almost stable state. Particularly, similar to the single-component models (see [43–48] and references therein), in the coupled optical media, the obtained new vector rogue waves may reveal another means to exert maximal control over a nonlinear system with minimal effort to produce highly stable supercontinuum, and the temporal and spatial-temporal breather solutions may be of significance for the applications of the coupled systems in spectroscopy, astronomy, navigation, or telecommunications. Similar to the idea [14,49], the method can also be used to generate the nonautonomous wave structures of the corresponding defocusing coupled NLS equations with varying coefficients and nonlocal coupled NLS equations. The results may excite the relevant experimental investigations in the Manakov-type optical and other media.

ACKNOWLEDGMENTS

The authors thank the referees for their variable comments and suggestions. This work was partially supported by the NSFC under Grants No. 11571346 and No. 61621003 and the Youth Innovation Promotion Association CAS.

[1] Y. S. Kivshar and G. P. Agrawal, *Optical Solitons: From Fibers to Photonic Crystals* (Academic Press, New York, 2003).
[2] G. P. Agrawal, *Nonlinear Fiber Optics*, 5th ed. (Academic Press, New York, 2013).
[3] B. A. Malomed, D. Mihalache, F. Wise, and L. Torner, J. Opt. B: Quantum Semiclassical Opt. **7**, R53 (2005); D. Mihalache, Rom. Rep. Phys. **69**, 403 (2017).
[4] V. E. Zakharov and A. B. Shabat, Sov. Phys.-JETP **34**, 62 (1972).
[5] H. Bailung and Y. Nakamura, J. Plasma Phys. **50**, 231 (1993).
[6] B. Kibler, J. Fatome, C. Finot, G. Millot, G. Genty, B. Wetzel, N. Akhmediev, F. Dias, and J. M. Dudley, Sci. Rep. **2**, 463 (2012).
[7] L. Pitaevskii and S. Stringari, *Bose-Einstein Condensation and Superfluidity* (Oxford University Press, Oxford, 2016).
[8] Z. Yan, Commun. Theor. Phys. **54**, 947 (2010).
[9] Z. Yan, Phys. Lett. A **375**, 4274 (2011).
[10] M. J. Ablowitz and P. A. Clarkson, *Solitons, Nonlinear Evolution Equations and Inverse Scattering* (Cambridge University Press, Cambridge, U.K., 1991).
[11] V. B. Matveev and V. Matveev, *Darboux Transformations and Solitons* (Springer-Verlag, New York, 1991).
[12] N. Akhmediev, A. Ankiewicz, and M. Taki, Phys. Lett. A **373**, 675 (2009).
[13] N. Akhmediev, A. Ankiewicz, and J. M. Soto-Crespo, Phys. Rev. E **80**, 026601 (2009).
[14] Z. Yan, Phys. Lett. A **374**, 672 (2010); Z. Yan, V. V. Konotop, and N. Akhmediev, Phys. Rev. E **82**, 036610 (2010); Z. Yan, J. Math. Anal. Appl. **380**, 689 (2011); Z. Yan and D. Jiang, *ibid.* **395**, 542 (2012); Z. Yan and C. Dai, J. Opt. **15**, 064012 (2013); Z. Yan, Nonlinear Dyn. **79**, 2515 (2015).
[15] V. Matveev, Phys. Lett. A **166**, 205 (1992).
[16] B. Guo, L. Ling, and Q. P. Liu, Phys. Rev. E **85**, 026607 (2012); J. S. He, H. R. Zhang, L. H. Wang, K. Porsezian, and A. S. Fokas, *ibid.* **87**, 052914 (2013); B. Guo, L. Tian, Z. Yan, and L. ling, *Rogue Waves and their Mathematical Theory* (Zhejiang Science and Technology, Hangzhou, China, 2015).
[17] X.-Y. Wen, Y. Yang, and Z. Yan, Phys. Rev. E **92**, 012917 (2015); X.-Y. Wen and Z. Yan, Commun. Nonlinear Sci. Numer. Simul. **43**, 311 (2017).
[18] X.-Y. Wen and Z. Yan, Chaos **25**, 123115 (2015); Y. Yang, Z. Yan, and B. A. Malomed, *ibid.* **25**, 103112 (2015); X.-Y. Wen, Z. Yan, and Y. Yang, *ibid.* **26**, 063123 (2016); X.-Y. Wen, Z. Yan, and B. A. Malomed, *ibid.* **26**, 123110 (2016); G. Zhang, Z. Yan, and Y. Chen, Appl. Math. Lett. **69**, 113 (2017).
[19] B. Guo and L. Ling, Chin. Phys. Lett. **28**, 110202 (2011).
[20] F. Baronio, A. Degasperis, M. Conforti, and S. Wabnitz, Phys. Rev. Lett **109**, 044102 (2012).
[21] F. Baronio, M. Conforti, A. Degasperis, S. Lombardo, M. Onorato, and S. Wabnitz, Phys. Rev. Lett. **113**, 034101 (2014).
[22] L. Ling, L. Zhao, and B. Guo, Commun. Nonlinear Sci. Numer. Simul. **32**, 285 (2016).
[23] P. Wai, C. R. Menyuk, and H. Chen, Opt. Lett. **16**, 1231 (1991).
[24] P. Wai and C. Menyak, J. Lightwave Technol. **14**, 148 (1996).
[25] C. R. Menyuk, IEEE J. Quantum Electron **QE-23**, 174 (1987).
[26] N. Lazarides and G. P. Tsironis, Phys. Rev. E **71**, 036614 (2005).
[27] M. Onorato, S. Residori, U. Bortolozzo, A. Montina, and F. Arecchi, Phys. Rep. **528**, 47 (2013).
[28] N. A. Kostov, V. Z. Enol'skii, V. S. Gerdjikov, V. V. Konotop, and M. Salerno, Phys. Rev. E **70**, 056617 (2004).
[29] V. A. Brazhnyi and V. V. Konotop, Phys. Rev. E **72**, 026616 (2005).
[30] D. J. Benney and A. C. Newell, Stud. Appl. Math. **46**, 133 (1967).
[31] S. V. Manakov, Sov. Phys.-JETP **38**, 248 (1974).
[32] J. Yang, Phys. D (Amsterdam, Neth.) **108**, 92 (1997).
[33] A. V. Porubov and D. F. Parker, Wave Motion **29**, 97 (1999).
[34] Y. S. Kivshar and S. K. Turitsyn, Opt. Lett. **18**, 337 (1993).
[35] C. R. Menyuk, IEEE J. Quantum Electron. **25**, 2674 (1989).
[36] J. U. Kang, G. I. Stegeman, J. S. Aitchison, and N. Akhmediev, Phys. Rev. Lett. **76**, 3699 (1996).
[37] Z. Chen, M. Segev, T. H. Coskun, D. N. Christodoulides, and Y. S. Kivshar, J. Opt. Soc. Am. B **14**, 3066 (1997).
[38] A. P. Sheppard and Y. S. Kivshar, Phys. Rev. E **55**, 4773 (1997).
[39] A. Degasperis and S. Lombardo, Phys. Rev. E **88**, 052914 (2013).
[40] L. Ling, L. Zhao, and B. Guo, Nonlinearity **28**, 3243 (2015).
[41] Q.-H. Park and H. Shin, Phys. D (Amsterdam, Neth.) **157**, 1 (2001).
[42] R. A. Horn and C. R. Johnson, *Matrix Analysis* (Cambridge University Press, Cambridge, U.K., 2012).

[43] L. A. Lugiato, IEEE J. Quantum Electron. **39**, 193 (2003).
[44] N. Akhmediev and A. Ankiewicz, *Dissipative Solitons: From Optics to Biology and Medicine* (Springer, New York, 2008).
[45] F. Leo *et al.*, Opt. Express **21**, 9180 (2013).
[46] M. Yu *et al.*, Nat. Commun. **8**, 14569 (2017).
[47] D. R. Solli, C. Ropers, P. Koonath, and B. Jalali, Nature (London) **450**, 1054 (2007).
[48] D. R. Solli, C. Ropers, and B. Jalali, Phys. Rev. Lett. **101**, 233902 (2008).
[49] Z. Yan, Appl. Math. Lett. **47**, 61 (2015); **62**, 101 (2016).